This is the accepted manuscript (postprint) of the following article:
Jazi, E. H., Esalmi-Farsani, R., Borhani, G., & Jazi, F. S. (2014). Synthesis and Characterization of In Situ Al-Al13Fe4-Al2O3-TiB2 Nanocomposite Powder by Mechanical Alloying and Subsequent Heat Treatment. *Synthesis and Reactivity in Inorganic, Metal-Organic, and Nano-Metal Chemistry*, *44*(2), 177-184. https://doi.org/10.1080/15533174.2013.768660

Synthesis and Characterization of In-Situ Al-$Al_{13}Fe_4$-Al_2O_3-TiB_2 Nanocomposite Powder by Mechanical Alloying and Subsequent Heat Treatment

E. Haghshenas Jazi[1], R. Esalmi-Farsani[1]*, Gh. Borhani[2], F. Sharifian Jazi[3]

[1] Department of Materials Engineering, Faculty of Mechanical Engineering, K. N. Toosi University of Technology, Tehran, Iran

[2] Department of Materials Engineering, Malek Ashtar University of Technology, Esfahan, Iran

[3] Mining and Metallurgical Engineering Department, Amirkabir University of Technology, Tehran, Iran

* Corresponding author: eslami@kntu.ac.ir

Abstract

Al-$Al_{13}Fe_4$-Al_2O_3-TiB_2 nanocomposite powder was fabricated by mechanical alloying (MA) and subsequent heat treatment of aluminum, ferrotitanium and boron oxide as a raw material. The obtained nanocomposite powder was evaluated by scanning electron microscopy (SEM) and X-ray diffraction (XRD). Also; microhardness values of powder particles after different milling times were measured. Microhardness of this nanocomposite was found to be about 161 HV. The results of XRD showed that the nanocrystalline supersaturated solid solutions of aluminum (α-Al) that formed within 30 h of MA with a mean crystallite size of 12 nm. The above experimental results showed that the heat treated 30 h of MA powders leads to the in situ formation of nanocrystalline TiB_2 in an Al matrix with a mean crystallite size of 45 nm. It was also found that after the heat treatment, moreover TiB_2 phase the other compound such as Al_2O_3 and $Al_{13}Fe_4$ have been formed.

Keywords: Nanocomposite, Al-TiB_2, Synthesis, Characterization, Mechanical alloying

1. Introduction

This is the accepted manuscript (postprint) of the following article:
Jazi, E. H., Esalmi-Farsani, R., Borhani, G., & Jazi, F. S. (2014). Synthesis and Characterization of In Situ Al-Al13Fe4-Al2O3-TiB2 Nanocomposite Powder by Mechanical Alloying and Subsequent Heat Treatment. *Synthesis and Reactivity in Inorganic, Metal-Organic, and Nano-Metal Chemistry*, *44*(2), 177-184. https://doi.org/10.1080/15533174.2013.768660

Aluminium metal matrix composites (MMC_s) are being considered as a group of advanced materials for their lightweight, high degree of chemical inertly, low coefficient of thermal expansion, high specific modulus, and good wear resistance properties (1,2). Mechanical properties of Al alloys can be greatly enhanced by incorporating reinforcing particles, forming composites (2). Among all particulate reinforced composites, the most interest is observed for those reinforced with hard ceramic particles, due to the possibility of controlling their mechanical properties by optimizing volume fraction, size, and distribution of the reinforcing particles in the matrix (3). A wide range of potential reinforcements have been considered, including SiC, Al_2O_3, SnO_2, B_4C, ZrO_2 and TiB_2 (4-9).

TiB_2 is compatible with aluminium matrix, and does not react with aluminium to form any reaction product at the interfaces of reinforcement and the matrix (10-12). On the other hand, TiB_2 is a refractory compound with many attractive properties, including exceptional hardness (approximately 25–35 GPa at room temperature, about three times harder than fully hardened structural steels), which is retained up to high temperatures. It has a high melting point (above 3000°C), good creep resistance, good thermal conductivity, high electrical conductivity, excellent wear and corrosion resistance, and considerable chemical stability (13-16). However, the formation of conventional TiB_2 is difficult and this is the major reason for its high cost and limited scope in engineering applications (17).

Composites reinforced by ceramic particles have been successfully fabricated by casting methods (18-20) and powder metallurgy (P/M) such as cryomilling (21, 22), ball milling (23) and wet mixing process (24). It is notable that some types of composites cannot be made by other alternative routes. Concerning aluminum matrix composites, P/M is one of the most widely used processing methods, due to its low processing costs coupled with its high versatility.

This is the accepted manuscript (postprint) of the following article:
Jazi, E. H., Esalmi-Farsani, R., Borhani, G., & Jazi, F. S. (2014). Synthesis and Characterization of In Situ Al-Al13Fe4-Al2O3-TiB2 Nanocomposite Powder by Mechanical Alloying and Subsequent Heat Treatment. *Synthesis and Reactivity in Inorganic, Metal-Organic, and Nano-Metal Chemistry*, *44*(2), 177-184.
https://doi.org/10.1080/15533174.2013.768660

In this research, the formation of Al-$Al_{13}Fe_4$-Al_2O_3-TiB_2 nanocomposite powder by MA and heat treatment was studied. For the first time, these inexpensive raw materials (Al, Ferrotitanium and B_2O_3) were used for synthesis of the nanocomposite. One aim of the work thus is to offer an inexpensive technique for fabrication of the nanocomposite.

2. Experimental

2.1. Materials

The starting materials used in this study included aluminium powder (Khorasan Powder Metallurgy Company, Iran, 99% purity, average particle size 45 μm), commercial grade ferrotitanium powder (Miller Company, England, 99.5% purity average particle size 80 μm), and B_2O_3 produced from commercial grade H_3BO_3 (PVT. LTD Company, India, 99.5% purity, average particle size 74 μm) at 900°C for 45 min by the reaction (1):

$$2H_3BO_3 \xrightarrow{\Delta} 3H_2O + B_2O_3 \quad (1)$$

To refine ferrotitanium powders were initially milled for 2 h. The composition of ferrotitanium determined by X-ray fluorescence (XRF) analyzer (Bruker, S4 PIONEER, Germany) is shown in Table 1.

Table 1. The composition of ferrotitanium

Elements	Fe	Ti	Al	V	C, S, P
Concentration (wt.%)	22.4	68.8	5	3.5	Balance

2.2. Sample Preparation

MA was performed using an attritor mill with a 2.5 L chromium steel vial and balls (AISI 52100) with a rotating speed of 585 rpm for 30 h under argon atmosphere. The ball to charge was chosen 10:1 and the diameters of the balls were 10 mm.

This is the accepted manuscript (postprint) of the following article:
Jazi, E. H., Esalmi-Farsani, R., Borhani, G., & Jazi, F. S. (2014). Synthesis and Characterization of In Situ Al-Al13Fe4-Al2O3-TiB2 Nanocomposite Powder by Mechanical Alloying and Subsequent Heat Treatment. *Synthesis and Reactivity in Inorganic, Metal-Organic, and Nano-Metal Chemistry*, *44*(2), 177-184. https://doi.org/10.1080/15533174.2013.768660

To reduce the excessive friction and increase mixing efficiency, 3 wt.% of stearic acid was added as a process control agent. This also avoided an excess of cold welding that could occur during the MA process. The temperature of the vial was kept close to ambient temperature with the aid of a water circulating system. Mechanically alloyed (MAed) powders were heat treated in a furnace with controlled argon atmosphere at 700 ± 5˚C for 1 h. The heat treated powders were furnace cooled.

2.3. Sample Characterization

2.3.1. XRD

Structural changes and phase transformation of powders during MA and following heat treatment were studied by XRD technique using a Cu K_α radiation (Philips PW 3710 diffractometer) at 40 kV and step size of 0.04° and a scan rate of 1 s. Nelson-Riley (NRF) method (25), used to calculate lattice parameter change in the Al matrix (equation 2):

$$\mathrm{NRF} = \frac{1}{2}\left(\frac{\cos^2\theta}{\sin\theta} + \frac{\cos^2\theta}{\theta}\right) \quad (2)$$

2.3.2. Microhardness Test

Microhardness of cross-section of powder particles was measured in a Wolpert Wilson Instruments 402MVD hardness tester under a load of 10 g for a dwelling time of 15 s and an average of five readings is reported.

2.3.3. SEM

Microstructure and phase investigation of mixed MAed and heat treated powders were carried out by SEM (VEGA II TESCAN-LMU) at an accelerating voltage of 15 Kv. In order to obtain high-resolution micrographs, gold coating was used during SEM characterization of

This is the accepted manuscript (postprint) of the following article:
Jazi, E. H., Esalmi-Farsani, R., Borhani, G., & Jazi, F. S. (2014). Synthesis and Characterization of In Situ Al-Al13Fe4-Al2O3-TiB2 Nanocomposite Powder by Mechanical Alloying and Subsequent Heat Treatment. *Synthesis and Reactivity in Inorganic, Metal-Organic, and Nano-Metal Chemistry*, *44*(2), 177-184. https://doi.org/10.1080/15533174.2013.768660

powders. Chemical composition at different locations was determined by X-ray energy dispersive spectroscopy (EDS) analysis.

3. Results and Discussion

3.1. Effect of Milling Time on XRD Patterns

Fig. 1 shows the XRD patterns of MA Al-Ferrotitanium-B_2O_3 powders after various milling times. It can be seen that Fe and Ti peaks are hardly observable, because of their low concentrations and partial overlapping of their peaks with the Al peaks.

A close examination of Fig. 1 reveals several interesting features: the peak position of Al reflections shifts to lower 2θ angles as the milling time increases, suggesting the formation of the Al-based solid solutions (α-Al) and an increase in the solute concentration as the milling time increases. As can be seen all aluminium reflections exhibit broadening and decrease in the peaks intensity by increasing milling times, indicating the grain size reduction and possibly the introduction of internal strains. As the milling time increases, the more broadening of XRD peaks is observed.

This is the accepted manuscript (postprint) of the following article:
Jazi, E. H., Esalmi-Farsani, R., Borhani, G., & Jazi, F. S. (2014). Synthesis and Characterization of In Situ Al-Al13Fe4-Al2O3-TiB2 Nanocomposite Powder by Mechanical Alloying and Subsequent Heat Treatment. *Synthesis and Reactivity in Inorganic, Metal-Organic, and Nano-Metal Chemistry*, *44*(2), 177-184.
https://doi.org/10.1080/15533174.2013.768660

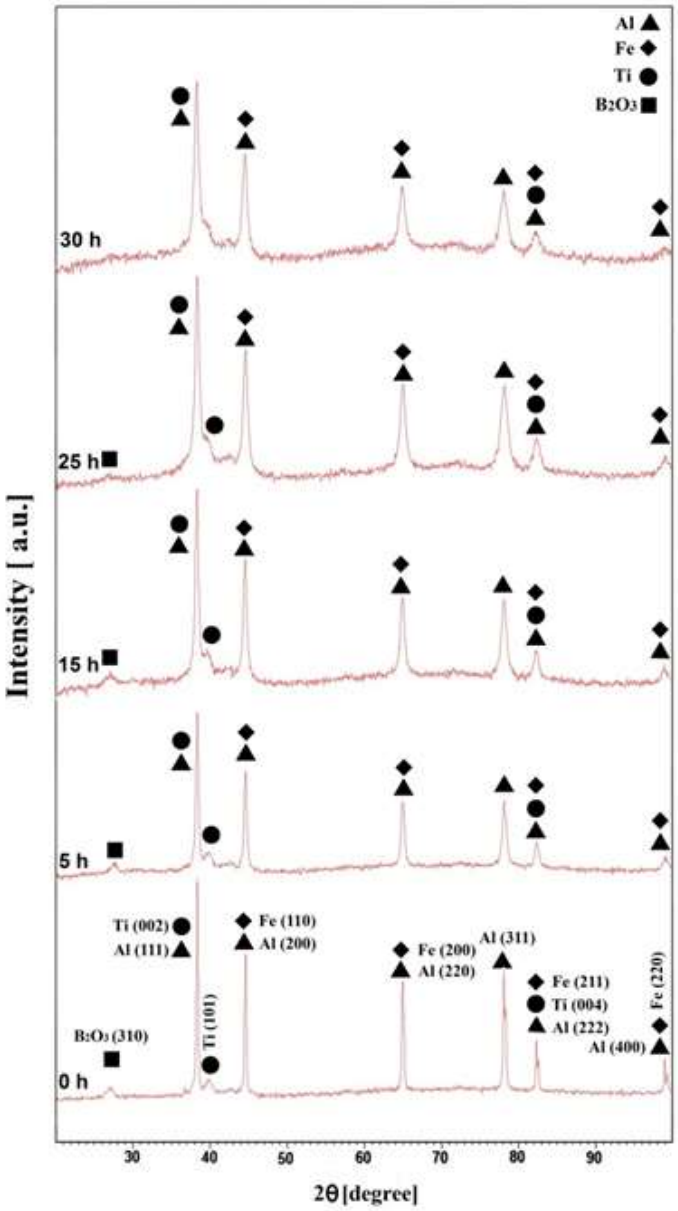

Figure 1. XRD patterns of MA Al-Ferrotitanium-B_2O_3 powder mixtures for different milling times.

Fig. 2 shows that with increasing milling times a small shift in the peak position of Al towards the lower diffraction angle, indicating an increase in the lattice parameter of the Al. The observed, increases in the lattice parameter are consistent with the possible formation of α-Al because the dissolution of Fe and Ti elements into fcc-Al. The atomic size of Fe element

This is the accepted manuscript (postprint) of the following article:
Jazi, E. H., Esalmi-Farsani, R., Borhani, G., & Jazi, F. S. (2014). Synthesis and Characterization of In Situ Al-Al13Fe4-Al2O3-TiB2 Nanocomposite Powder by Mechanical Alloying and Subsequent Heat Treatment. *Synthesis and Reactivity in Inorganic, Metal-Organic, and Nano-Metal Chemistry*, *44*(2), 177-184.
https://doi.org/10.1080/15533174.2013.768660

is smaller than that of the Al element, whereas the atomic size of the Ti element is larger to that of the Al element (26, 27). Dissolution of Fe and Ti in Al leads to solid solution, which promotes easy fragmentation of the powder particles during MA, and thus refining the crystallites [28). MA has been used for the synthesis of several intermetallic phases in both the disordered and ordered conditions. In many cases the intermetallic were synthesized directly by MA, but in others an additional heat treatment was required after MA to form the intermetallic. The intermetallic synthesized includes aluminides, borides, carbides, nitrides, and silicides [29).

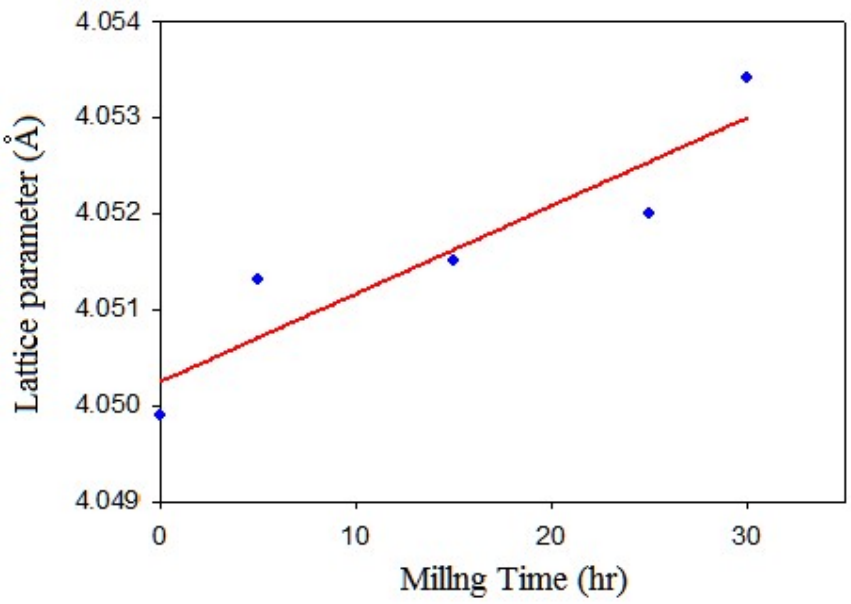

Figure 2. Variation of lattice parameter of MAed powders with duration of MA.

3.2. Effect of Heat Treatment on XRD Patterns

Fig. 3 shows the XRD patterns of MA Al-Ferrotitanium-B_2O_3 powders after 15 and 30 h of milling and subsequent heat treatment. As seen in Fig. 3(a), after heat-treating, $Al_{13}Fe_4$ and Al_2O_3 peaks appear, but no TiB_2 peaks are detected. Nayak, et al. (28), reported that MA of dilute Al–Fe alloys containing 2.5–10 at.% Fe for 20 h resulted in the formation of α-Al, but

This is the accepted manuscript (postprint) of the following article:
Jazi, E. H., Esalmi-Farsani, R., Borhani, G., & Jazi, F. S. (2014). Synthesis and Characterization of In Situ Al-Al13Fe4-Al2O3-TiB2 Nanocomposite Powder by Mechanical Alloying and Subsequent Heat Treatment. *Synthesis and Reactivity in Inorganic, Metal-Organic, and Nano-Metal Chemistry*, *44*(2), 177-184.
https://doi.org/10.1080/15533174.2013.768660

heat treatment at high temperature, i.e., 500°C enabled α-Al to precipitate out $Al_{13}Fe_4$ intermetallic. Lee, et al. reported that the major product of the Al–Fe reaction can be identified as $Al_{13}Fe_4$ (also denoted as Al_3Fe); however, formation of minor amounts of Al_5Fe_2 was also seen (29).

TiB_2 has formed after 30 h of milling and thus several peaks of this phase appeared in the XRD pattern as shown in Fig. 3(b). The other compounds such as $Al_{13}Fe_4$ and Al_2O_3 were also observed on the XRD patterns after heat-treating process. It can be seen, that the intensity of the Al reflections increases with the increase in milling time and shifts to higher diffraction angle, suggesting the formation of a new phases, at the expense of α-Al solid solution after heat-treating.

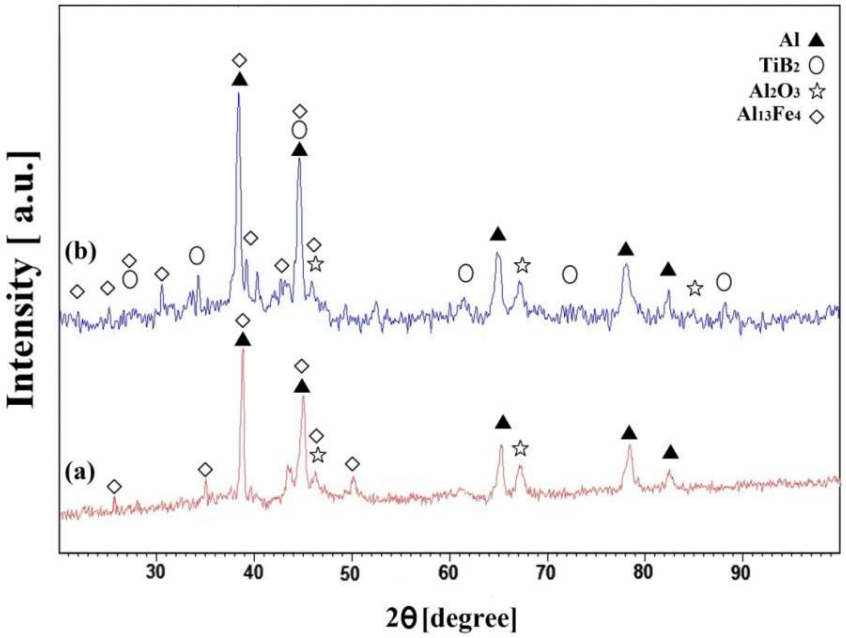

Figure 3. XRD patterns of MA Al-Ferrotitanium-B_2O_3 powders and subsequent heat treatment at 700°C for 1h: (a) 15 h MA, (b) 30 h MA.

This is the accepted manuscript (postprint) of the following article:
Jazi, E. H., Esalmi-Farsani, R., Borhani, G., & Jazi, F. S. (2014). Synthesis and Characterization of In Situ Al-Al13Fe4-Al2O3-TiB2 Nanocomposite Powder by Mechanical Alloying and Subsequent Heat Treatment. *Synthesis and Reactivity in Inorganic, Metal-Organic, and Nano-Metal Chemistry*, *44*(2), 177-184. https://doi.org/10.1080/15533174.2013.768660

The peak position of the Al reflections has shifted to higher 2θ angles as the milling time has increased; this implies that during heat treatment the lattice parameter of the Al has decreased. However, after powders MA for 30 h and heat-treating the lattice parameter (0.40512 nm) is still is more than of pure Al (0.40496 nm). The grain size of the aluminium matrix and TiB_2 was obtained from XRD analysing data using Williamson–Hall (WH) equation (3) (25):

$$\beta \cos\theta = \frac{0.9\lambda}{d} + 4\varepsilon \sin\theta \quad (3)$$

Where, β is the full width at half maximum (FWHM) of the Bragg peaks (in radians), θ is the Bragg angle of the analysed peak, λ is the wavelength of the X-rays used in nanometers (0.154056 nm for Cu Kα), d is the average crystallite size, and ε is the average internal strain. The average internal strain can be estimated from the linear slope of β cos θ versus sin θ, while the average crystallite size can be estimated from intersect of this line at sin θ = 0. The average crystallite size average internal strain of the Al matrix and TiB_2 particles after various milling times are reported in Table 2. The grain size of TiB_2 particles formed after heat-treating was measured to be about 16 nm. In expense of TiB_2 formation the Al grain size has increased from 12 nm to about 45 nm.

Table 2. Average crystallite size calculated by WH method for various milling times

Sample	Crystalline size (nm)	
	Al	TiB_2
15 h MA	82	-
25 h MA	24	-
30 h MA	12	-
12 h MA and heat treatment at 700˚C	> 100	-
30 h MA and heat treatment at 700˚C	45	16

This is the accepted manuscript (postprint) of the following article:
Jazi, E. H., Esalmi-Farsani, R., Borhani, G., & Jazi, F. S. (2014). Synthesis and Characterization of In Situ Al-Al13Fe4-Al2O3-TiB2 Nanocomposite Powder by Mechanical Alloying and Subsequent Heat Treatment. *Synthesis and Reactivity in Inorganic, Metal-Organic, and Nano-Metal Chemistry*, *44*(2), 177-184. https://doi.org/10.1080/15533174.2013.768660

3.3. Phase Evolution and Reaction Mechanism

It is well known that MA introduces large amount of defects such as vacancies, dislocations and grain boundaries into the milled powders. In the MAed powder, the degree lattice deformation is high or the degree of lattice ordering is low, which indicates that the powder is in non-equilibrium state. Heat treatment of milled powders causes some recovery in structural defects. Atoms in the disordered or distorted positions rearrange and/or move into more thermodynamically equilibrated and ordered or perfect lattice positions, enhancing the degree of ordering and strain release in the matrix. The heat-treating of the MAed powder favours the diffusivity of Fe, Ti and Al. Meanwhile, the Ti and B precipitate from the non-equilibrium supersaturated Al (Fe, Ti, B) solid solution, and react to form hexagonal TiB_2 compound (30). Therefore, probably in this work heat treatment results in the phase transformation from Al (Fe, Ti) into intermetallic $Al_{13}Fe_4$ and TiB_2 compounds (equation 4):

$$\mathrm{Al\ (Fe, Ti)} \rightarrow \mathrm{Al_{13}Fe_4 + TiB_2} \quad (4)$$

Ma, et al. indicted that in the Al–TiO_2–B_2O_3 system after the thermite reactions between Al and metal oxides, the reduced Ti will react with B to form TiB_2 (31).

TiB_2 cannot be directly formed from the reduction of B_2O_3 in the presence of Ti since B_2O_3 has much lower Gibbs free energy than that of TiB_2 (32). Therefore, the formation mechanism of TiB_2 can be suggested to involve two steps. In the first step, the oxygen atoms may be reduced by the displacement of oxygen atoms from B_2O_3 so that B atoms can be freed by the formation of Al_2O_3, since the Gibbs free energy of Al_2O_3 is much lower than that of B_2O_3, equation (5):

$$\mathrm{2Al + B_2O_3 \rightarrow Al_2O_3 + 2B} \quad (5)$$

In second step of the reaction, the released heat for exothermic reaction (5) provides the activation energy for reaction of Ti with B in the matrix (equations 6):

This is the accepted manuscript (postprint) of the following article:
Jazi, E. H., Esalmi-Farsani, R., Borhani, G., & Jazi, F. S. (2014). Synthesis and Characterization of In Situ Al-Al13Fe4-Al2O3-TiB2 Nanocomposite Powder by Mechanical Alloying and Subsequent Heat Treatment. *Synthesis and Reactivity in Inorganic, Metal-Organic, and Nano-Metal Chemistry*, *44*(2), 177-184. https://doi.org/10.1080/15533174.2013.768660

$$Ti + 2B \rightarrow TiB_2 \quad (6)$$

3.4. Microstructural and Morphological Studies

During the ball milling process, particles are repeatedly flattened, fractured and welded. Fracture and welding are the two basic events which produce a permanent exchange of matter between particles and

ensure mixing of the various elements of ground powders. The processes of cold welding and fracturing, as well as their kinetics and predominance at any stage, depend mostly on the deformation characteristics of the starting powders.

Fig. 4 shows the SEM images of as-milled and 30 h milled powders. The milling of time has caused an increase in work hardening of Al powders, excess of fracturing and as a result the size of powder particles decreased. Also, after 30 h of milling no free particles were found, that means all the particles have been incorporated to the Al matrix, imply to a full composite powder. As can be seen in Fig. 4b, distribution of particles is uniformed after 30 h of milling. Then, the mentioned of milling time is the optimum to formation of the α-Al. The average particle size of MA powders before heat treatment is about 1-8 μm.

This is the accepted manuscript (postprint) of the following article:
Jazi, E. H., Esalmi-Farsani, R., Borhani, G., & Jazi, F. S. (2014). Synthesis and Characterization of In Situ Al-Al13Fe4-Al2O3-TiB2 Nanocomposite Powder by Mechanical Alloying and Subsequent Heat Treatment. *Synthesis and Reactivity in Inorganic, Metal-Organic, and Nano-Metal Chemistry*, *44*(2), 177-184. https://doi.org/10.1080/15533174.2013.768660

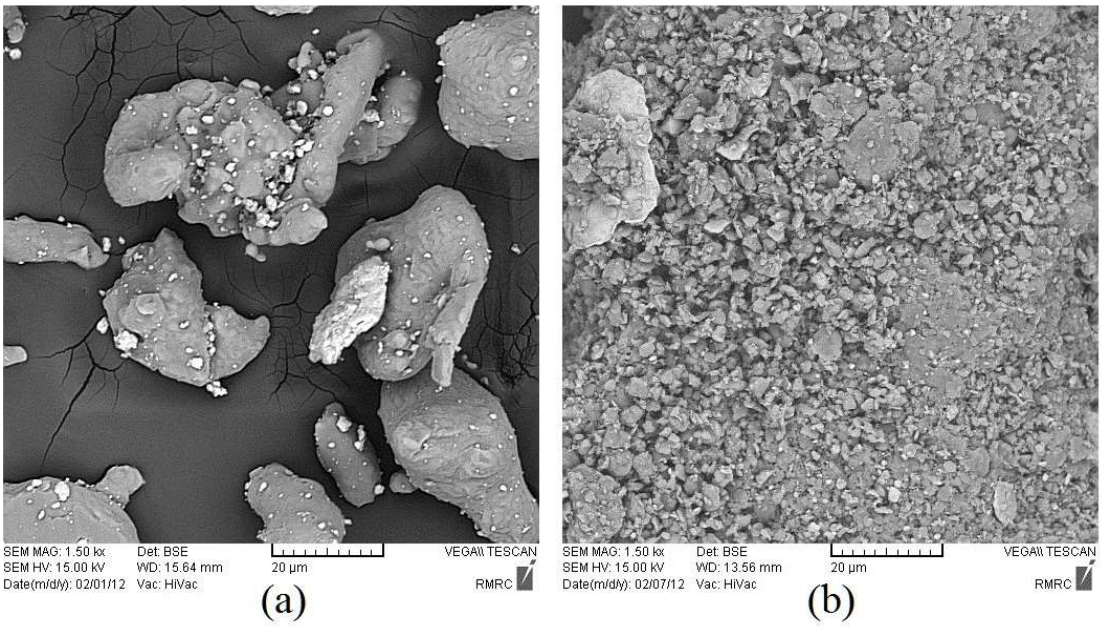

Fig. 4. SEM morphology and distribution of particles: (a) as-milled, (b) 30 h milled Al-Ferrotitanium-B_2O_3 powders.

EDS was performed on the marked particles (A and B) in Fig. 5. The results of this analysis were shown presence of Al, Ti, Fe, and O. The results of revealed that Ti and Fe atoms penetrate deep from the surface into the interior regions of Al particles. Therefore, the elements become dissolved in the whole Al volume, leading to the formation of Al (Ti, Fe) solid solution that is in agreement with XRD results (Fig. 1).

This is the accepted manuscript (postprint) of the following article:
Jazi, E. H., Esalmi-Farsani, R., Borhani, G., & Jazi, F. S. (2014). Synthesis and Characterization of In Situ Al-Al13Fe4-Al2O3-TiB2 Nanocomposite Powder by Mechanical Alloying and Subsequent Heat Treatment. *Synthesis and Reactivity in Inorganic, Metal-Organic, and Nano-Metal Chemistry*, *44*(2), 177-184. https://doi.org/10.1080/15533174.2013.768660

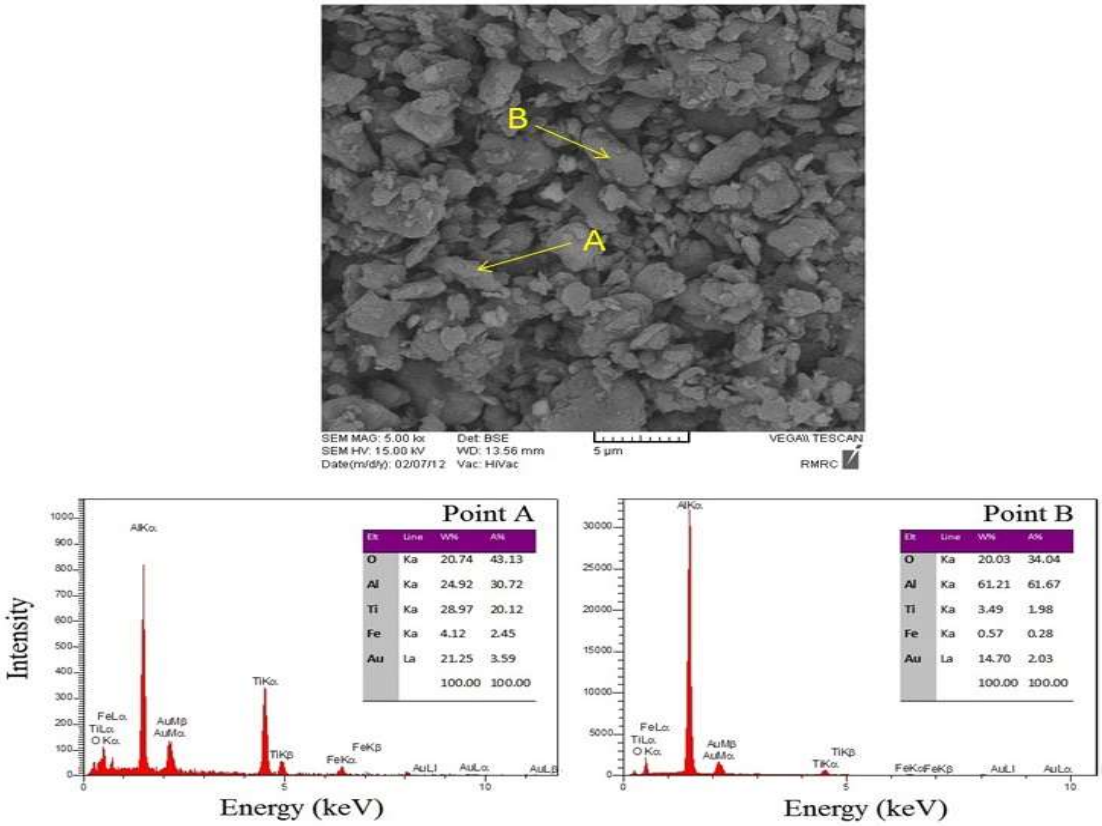

Fig. 5. SEM morphology and EDS results of chemical compositions for point A and B of 30 h milled powder before heat treating.

However, after heat-treating, it is clear that the agglomerate particles which were obtained after prolonged milling time (30 h) come into contact and form small agglomerates and coarser particles as shown in Figs. 6a and 6b. The average powder particle size after heat-treating is about 3-5 µm. There are the Al, Ti, Fe, and O reflections in the EDS analysis that confirm compositions of heat treated powder. Theses compositions were estimated to be Al, TiB_2, Al_2O_3, and $Al_{13}Fe_4$ at point A, B, C, and D, respectively. Boron reflections cannot be analyzed by this method. The XRD patterns confirmed the presence of the compounds in the powders (Fig. 3).

This is the accepted manuscript (postprint) of the following article:
Jazi, E. H., Esalmi-Farsani, R., Borhani, G., & Jazi, F. S. (2014). Synthesis and Characterization of In Situ Al-Al13Fe4-Al2O3-TiB2 Nanocomposite Powder by Mechanical Alloying and Subsequent Heat Treatment. *Synthesis and Reactivity in Inorganic, Metal-Organic, and Nano-Metal Chemistry*, *44*(2), 177-184. https://doi.org/10.1080/15533174.2013.768660

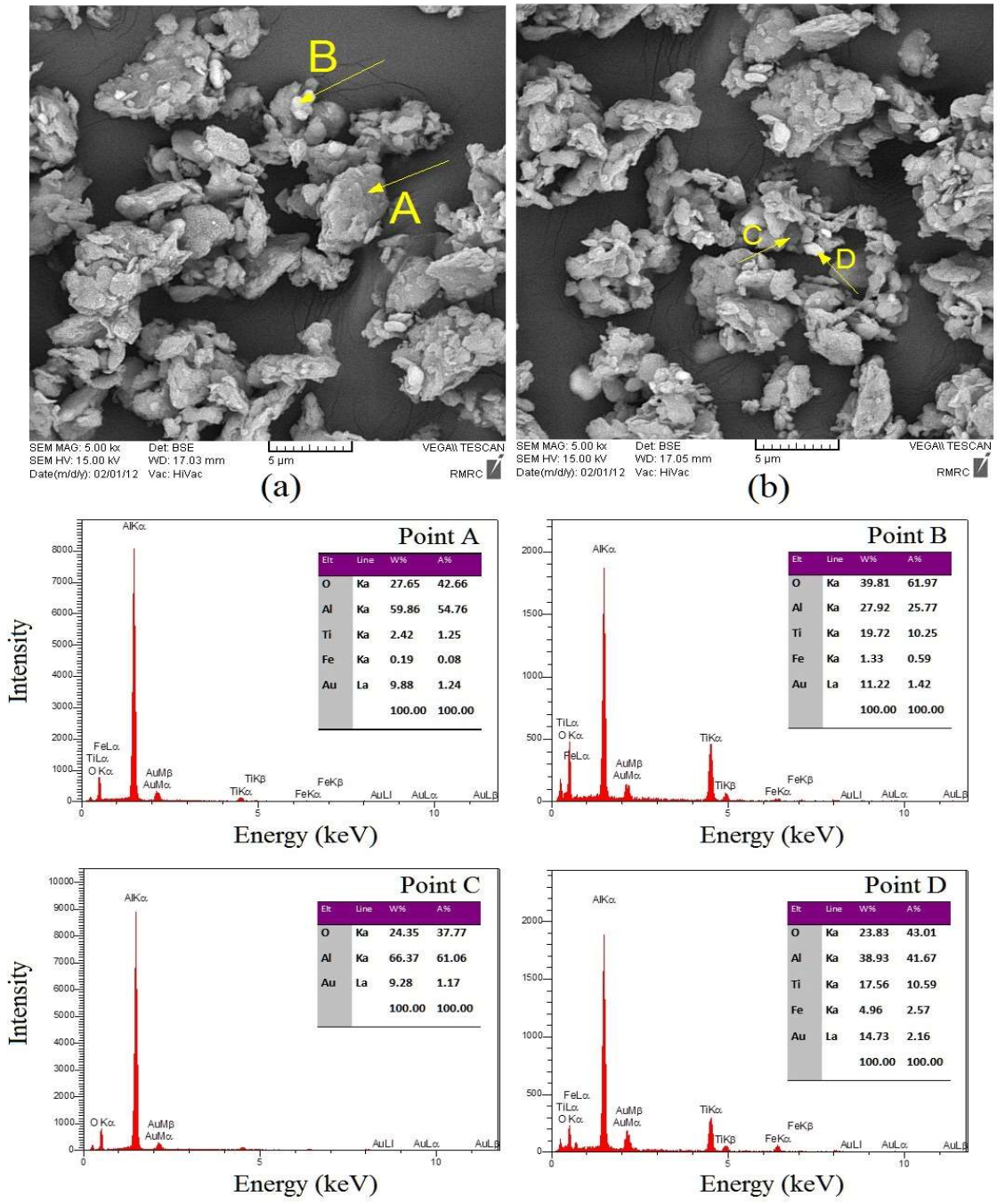

Fig. 6. SEM morphology and EDS results of chemical compositions for point A, B, C and D of 30 h milled powder after heat treating.

3.5. Morphological Changes

This is the accepted manuscript (postprint) of the following article:
Jazi, E. H., Esalmi-Farsani, R., Borhani, G., & Jazi, F. S. (2014). Synthesis and Characterization of In Situ Al-Al13Fe4-Al2O3-TiB2 Nanocomposite Powder by Mechanical Alloying and Subsequent Heat Treatment. *Synthesis and Reactivity in Inorganic, Metal-Organic, and Nano-Metal Chemistry*, *44*(2), 177-184. https://doi.org/10.1080/15533174.2013.768660

Fig. 7 shows the variation in average particle size during the MA. In the initial stages of milling, considerable decrease in average particle size is a result of milling Al coarse powder particles. Science Al particles are subjected to compressive impact forces and undergo plastic deformation, therefore metal powder particles get flattened but welding of soft powder particles has not occurred (33). By increasing milling time, work hardening happens and consequently due to and increased brittleness of powder, particle size continuously decreases. This decrease can happen mostly in the first 15 h of the milling process.

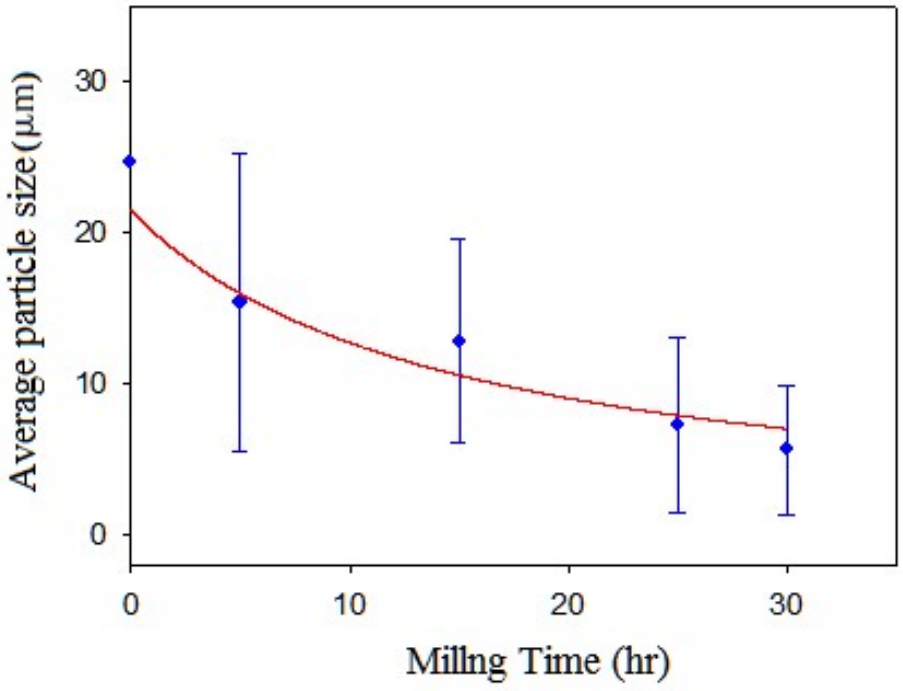

Fig. 7. The average powder particle size for various milling time.

3.6. Microhardness Measurements

Microhardness values of powder particles after different milling times are shown in Fig. 8. As can be seen, increasing milling times led to gradually increase powder hardness. The increase in hardness value due to the plastic deformation induced during MA. In this situation

This is the accepted manuscript (postprint) of the following article:
Jazi, E. H., Esalmi-Farsani, R., Borhani, G., & Jazi, F. S. (2014). Synthesis and Characterization of In Situ Al-Al13Fe4-Al2O3-TiB2 Nanocomposite Powder by Mechanical Alloying and Subsequent Heat Treatment. *Synthesis and Reactivity in Inorganic, Metal-Organic, and Nano-Metal Chemistry*, *44*(2), 177-184.
https://doi.org/10.1080/15533174.2013.768660

work hardening, fine grain size, contributing elements, and the solute atoms are occurred in the powders. As seen in Fig. 8, up to 15 h, microhardness increases rapidly to 154 HV and at longer milling times the increasing trend continues with a slower rate to 162 HV for 30 h. From 15 to 30 h, slower rate of increase of microhardness probably can be attributed to reach the steady state MA and dynamic recovery by high work hardening effect of deformed matrix (34).

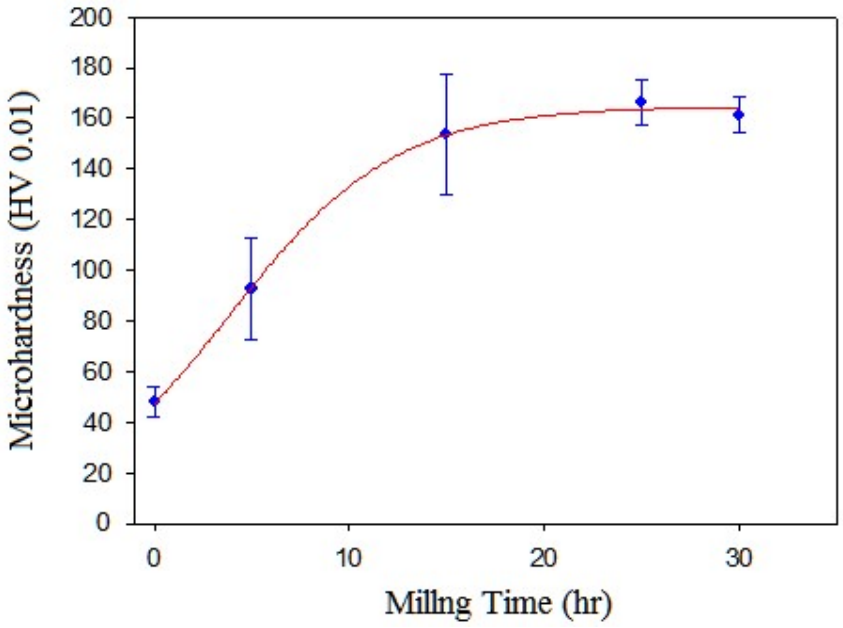

Fig. 8. Microhardness values of cross-section of powder particles for various milling times.

4. Conclusions

From the microstructure and microhardness changes of Al-$Al_{13}Fe_4$-$Al2O_3$-TiB_2 nanocomposite powder during MA and subsequent heat treatment the following conclusions could be drown:

This is the accepted manuscript (postprint) of the following article:
Jazi, E. H., Esalmi-Farsani, R., Borhani, G., & Jazi, F. S. (2014). Synthesis and Characterization of In Situ Al-Al13Fe4-Al2O3-TiB2 Nanocomposite Powder by Mechanical Alloying and Subsequent Heat Treatment. *Synthesis and Reactivity in Inorganic, Metal-Organic, and Nano-Metal Chemistry*, *44*(2), 177-184. https://doi.org/10.1080/15533174.2013.768660

1- The MA method and heat treatment process of Al, ferrotitanium and B_2O_3 powders have been successfully employed to synthesis of Al-$Al_{13}Fe_4$-Al_2O_3-TiB_2 nanocomposite powders.

2- The Al-based solid solutions (α-Al) formed after 30 h milling time due to solution of Ti and Fe in the Al matrix, which promotes easy fragmentation of the powder particles during MA, and thus refining the crystallites.

3- By milling for 30 h, the crystallite size has decreased to 12 nm but after heat treating for 1 h at 700 ºC the crystallite size has increased to 45 nm.

4- After 30 h of milling, the lattice parameter of Al has increases to 0.40534 nm and has decreased to 0.40512 nm after heat-treating at 700˚C.

5- Microhardness of the milling powder after 30 h increases to about 162 HV.

References

[1] J.W. Kaczmar, K. Pietrzak, W. Wlosinski, The production and application of metalmatrix composite materials, *J Mater Process Technol* 2000; 106: 58–67.

[2] H.Y. Wang, Q.C. Jiang, Y. Wang, B.X. Ma, F. Zhao, Fabrication of TiB_2 particulate reinforced magnesium matrix composites by powder metallurgy, *Mater Lett* 2004; 58: 3509–3513.

[3] T.R. Chapman, D.E. Niesz, R.T. Fox, T. Fawcett, Wear-resistant aluminum–boron–carbide cermets for automotive brake applications, *Wear* 1999; 236: 81–88.

[4] M. Bermudez, F.J. Carrion, P. Iglesias, G. Martinez-Nicolas, E.J. Herrera, J.A. Rodriguez, Influence of milling conditions on the wear resistance of mechanically alloyed aluminum, *Wear* 2005; 258: 906–914.

[5] M. Alizadeh, M.H. Paydar, F. Sharifian Jazi, Structural evaluation and mechanical properties of nanostructured Al/B_4C composite fabricated by ARB process, *Compos Part B-Eng,* Article in press.

[6] R, Ekici, M.K, Apalak, M. Yildirim, Indentation behavior of functionally graded Al–SiC metal matrix composites with random particle dispersion, *Compos Part B-Eng*, 2011; 42: 1497–1507.

This is the accepted manuscript (postprint) of the following article:
Jazi, E. H., Esalmi-Farsani, R., Borhani, G., & Jazi, F. S. (2014). Synthesis and Characterization of In Situ Al-Al13Fe4-Al2O3-TiB2 Nanocomposite Powder by Mechanical Alloying and Subsequent Heat Treatment. *Synthesis and Reactivity in Inorganic, Metal-Organic, and Nano-Metal Chemistry*, *44*(2), 177-184. https://doi.org/10.1080/15533174.2013.768660

[7] S. Gopalakrishnan, N. Murugan, Production and wear characterisation of AA 6061matrix titanium carbide particulate reinforced composite by enhanced stir casting method, *Compos Part B-Eng,* Article in press.

[8] Z. Zhou, Z. Wang, Y. Yi, S. Jiang, G. Wang, J. Chen, Properties and micro-structure of ZrO_2–Al_2O_3 composites with three-layer structure, *Compos Part B-Eng* 2011; 42: 1271–1275.

[9] F. Sharifian Jazi, N. Parvin, A. R. Azadmehr, M. Tahriri, Influence of annealing temperature on distribution and morphology of silver powder in SnO_2-Ag_2O nanocomposite, *Adv Appl Ceram*, Article in press.

[10] M. Zhao, G. Wu, Z. Dou, L. Jiang, TiB_{2P}/Al composite fabricated by squeeze casting technology, *Mater. Sci. Eng*. A, 2004; 374: 303–306.

[11] M. Emamy, M. Mahta, J. Rasizadeh, Formation of TiB_2 particles during dissolution of $TiAl_3$ in Al–TiB_2 metal matrix composite using an in situ technique, *Compos. Sci. Technol*, 2006; 66: 1063–1066.

[12] R. Sachan, J.W. Park, Formation of nanodispersoids in Fe–Cr–Al/30%TiB_2 composite system during mechanical alloying, *Alloys Comp*, 2009; 485: 724–729.

[13] H.B. Lee, S.H. Kim, S.W. Kang, Y.H. Han, Characterisation of mechanically alloyed Ti–Al–B nanocomposite consolidated by spark plasma sintering, *J. Korean Ceram. Soc*, 2008; 45: 815–820.

[14] K.L. Tee, L. Lu, M.O. Lai, Synthesis of in situ Al-TiB_2 composites using stir cast route, *Compos. Struct*, 1999; 47: 589–593.

[15] Z.Y. Chen, Y.Y. Chen, Q. Shu, G.Y. An, D. Li, Y.Y. Liu, Microstructure and properties of in situ Al/TiB_2 composite fabricated by in-melt reaction method, *Metall. Mater. Trans*. A, 2000; 31: 1959.

[16] A. Jain, R. Pankajavalli, S. Anthonysamy, Determination of the thermodynamic stability of TiB_2, *J. Alloys Compd*, 2010; 491: 747–752.

[17] J.S. Peters, B.A. Cook, J.L. Harringa, A.M. Russell, Microstructure and wear resistance of low temperature hot pressed TiB_2, *Wear*, 2009; 266: 1171–1177.

[18] K.M. Shorowordi, A. Haseeb, J.P. Celis, Tribo-surface characteristics of Al–B4C and Al–SiC composites worn under different contact pressures, *Wear* 2006; 261:634–641.

[19] D.L. Chung, Composite Materials: Functional Materials for Modern Technologies, Springer, London, 2003.

[20] T.S, Srivatsan, I.A. Ibrahim, F.A. Mohamed, E.J. Lavernia, Processing techniques for particulate-reinforced metal aluminium matrix composites, *J Mater Sci* 1991; 265: 965-975.

[21] H.S. Lee, J.S. Yeo, S.H. Hong, D.J. Yoon, The fabrication process and mechanical properties of SiCp/Al–Si metal matrix composites for automobile air-conditioner compressor pistons, *J Mater Process Technol* 2001; 113: 202-208.

[22] G. Ganesan, K. Raghukandan, R. Karthikeyan, Development of processing maps for 6061 Al/15% SiC_p composite material, *Mater Sci Eng. A,* 2004; 369: 230-235.

[23] M. Alizadeh, M.H. Paydar, Fabrication of nanostructure Al/SiC_P composite by accumulative roll-bonding (ARB) process, *J Alloys Compd,* 2010; 492: 231-235.

[24] R.Z. Abdulov, R.Z. Valiev, N.A. Krasilnikov, Formation of submicrometre-grained structure in magnesium alloy due to high plastic strains, *J Mater Sci Lett,* 1990; 9: 1445-1447.

[25] B.D. Cullity, Elements of X-ray Diffraction, 2nd edn.; Addison-Wesley, Boston, MA, 1978.

[26] M. Zawrah, L. Shaw, Microstructure and hardness of nanostructured Al-Fe-Cr-/Ti alloys through mechanical alloying, *Mater. Sci. Eng. A,* 2003; 355: 37–49.

[27] F.G. Cuevas, J. Cintas, J.M. Montes, J.M. Gallardo, Al–Ti powder produced through mechanical alloying for different times, *J. Mater. Sci,* 2006; 41: 8339–8346.

[28] S.S. Nayaka, M. Wollgartenb, J. Banhartb, S.K. Pabia, B.S Murtyc, Nanocomposites and an extremely hard nanocrystalline intermetallic of Al–Fe alloys prepared by mechanical alloying, *Mater. Sci. Eng. A,* 2010; 527: 2370–2378.

[29] I.S. Lee, P.W. Kao, N.J. Ho, Microstructure and mechanical properties of Al–Fe in situ nanocomposite produced by friction stir processing, *Intermet,* 2008; 16: 1104–1108.

[30] R. Ren, Y. Wu, W. Tang, F. Wang, T. Wang, Z. Zheng, Synthesis and grain growth kinetics of in-situ FeAl matrix nanocomposites (II): structural evolution and grain growth kinetics of mechanically alloyed Fe-Al-Ti-B composite powder during heat treatment, *Trans. Nonferrous Met. Soc. China*, 2008; 18: 66–71.

[31] Z.Y. Ma, S.C. Tjong, In situ ceramic particle-reinforced aluminium matrix composites fabricated by reaction pressing in the TiO2 (Ti)–Al–B (B2O3) systems, *Metall. Mater. Trana. A,* 1997; 28: 1931–1942.

[32] E.M. Sharifi, F. Karimzadeh, M.H. Enayati, Preparation of Al_2O_3–TiB_2 nanocomposite powder by mechanochemical reaction between Al, B_2O_3 and Ti, *Adv. Powder Technol,* 2011; 22: 526–531

This is the accepted manuscript (postprint) of the following article:
Jazi, E. H., Esalmi-Farsani, R., Borhani, G., & Jazi, F. S. (2014). Synthesis and Characterization of In Situ Al-Al13Fe4-Al2O3-TiB2 Nanocomposite Powder by Mechanical Alloying and Subsequent Heat Treatment. *Synthesis and Reactivity in Inorganic, Metal-Organic, and Nano-Metal Chemistry*, *44*(2), 177-184. https://doi.org/10.1080/15533174.2013.768660

[33] A. T. Chaharsoughi, Gh. Borhani, R. Tahmasebi, Structural characterization of $MoSi_2$ synthesized by high-energy mechanical milling followed by annealing heat treatment, *J. Alloys Compd*, 2011; 509: 2617–2620.

[34] C. Suryanarayana, Mechanical alloying and milling, *Prog Mater Sci,* 2001; 46:1-184.